

High-sensitive terahertz parametric upconversion detection up to 6 THz in KTP crystal

Yu-Ye Wang(王与烨), Zi-Kun Liu(刘紫鲲), Xu-Bing Feng(徐炳烽), Jing-Xi Zhang(张敬喜), Hong-Ru Ma(马鸿儒), De-Gang Xu(徐德刚), Jian-Quan Yao(姚建铨)

Citation: Chin. Phys. B. 35, 094208 (2026). DOI: 10.1088/1674-1056/ae1c28 | CSTR:32038.14.CPB.ae1c28

http://cpb.iphy.ac.cn; http://iopscience.iop.org/cpb

What follows is a list of articles you may be interested in

Dynamic control of topological phase of Dirac semimetallic terahertz metasurface

Chenglong Wang(王成龙), Zhihua Han(韩志华), Xiang Hou(侯翔), Yansheng Shao(邵延胜), Fangze Deng(邓方泽), Keke Cheng(程可可), Yuchao Li(李玉超), Ke Ma(马克), Yumeng Ma(马宇萌), Huiyun Zhang(张会云), Meng Liu(刘蒙), Yuping Zhang(张玉萍)

Chin. Phys. B. 35, 034207 (2026). DOI: 10.1088/1674-1056/adfbd8 | CSTR: 32038.14.CPB.adfbd8

Ultra-broadband and wide-angle reflective terahertz polarization conversion metasurface based on topological optimization

Ya-Jie Zhang(张亚杰), Chao-Long Li(李潮龙), Jia-Qi Luan(栾迦淇), Ming Zhao(赵茗), Ding-Shan Gao(郜定山), Pei-Li Li(李培丽)

Chin. Phys. B. 33, 104210 (2024). DOI: 10.1088/1674-1056/ad5d91

Enhanced picosecond terahertz wave generation based on cascade effects in a terahertz parametric generator

Jingxi Zhang(张敬喜), Yuye Wang(王与烨), Bingfeng Xu(徐炳烽), Kai Chen(陈锴), Zikun Liu(刘紫鲲), Hongru Ma(马鸿儒), Degang Xu(徐德刚), Jianquan Yao(姚建铨)

Chin. Phys. B. 33, 084203 (2024). DOI: 10.1088/1674-1056/ad47b0

Multi-channel terahertz focused beam generator based on shared-aperture metasurface

Jiu-Sheng Li(李九生), Yi Chen(陈翊)

Chin. Phys. B. 32, 124204 (2023). DOI: 10.1088/1674-1056/acddd2

Terahertz shaping technology based on coherent beam combining

Xiao-Ran Zheng(郑晓冉), Dan-Ni Ma(马丹妮), Guang-Tong Jiang(蒋广通), Cun-Lin Zhang(张存林), Liang-Liang Zhang(张亮亮)

Chin. Phys. B. 32, 114210 (2023). DOI: 10.1088/1674-1056/acc2b0

High-sensitive terahertz parametric upconversion detection up to 6 THz in KTP crystal

Yu-Ye Wang(王与烨)[1,2,†], Zi-Kun Liu(刘紫鲲)[1,2], Bing-Feng Xu(徐炳烽)[1,2], Jing-Xi Zhang(张敬喜)[1,2], Hong-Ru Ma(马鸿儒)[1,2], De-Gang Xu(徐德刚)[1,2], and Jian-Quan Yao(姚建铨)[1,2]

[1] *School of Precision Instruments and Optoelectronics Engineering, Tianjin University, Tianjin* 300072, *China*
[2] *Key Laboratory of Optoelectronic Information Technology (Ministry of Education), Tianjin University, Tianjin* 300072, *China*

(Received 13 October 2025; revised manuscript received 1 November 2025; accepted manuscript online 6 November 2025)

A highly sensitive terahertz (THz) wave parametric upconversion detector was demonstrated based on $KTiOPO_4$ (KTP) crystal pumped by a nanosecond 1064-nm laser. The effects of pump energy on the detection sensitivity were studied in this experiment, where the upconversion signal and spontaneous noise were both amplified linearly with the increase of pump energy. The minimum detectable THz wave energy of 57.6 aJ was realized at 5.74 THz under higher pump energy, which gives the dynamic range of 104 dB and noise equivalent power (NEP) of 147.8 fW/Hz$^{1/2}$. It was three orders of magnitude higher than that of bolometer. Moreover, a rapid-response detection in the THz frequency range of 5.24 THz–6.14 THz was achieved. This THz parametric upconversion detector based on KTP crystal can provide a technical solution to achieve high-sensitive THz detection in a wide THz region.

Keywords: terahertz wave, parametric upconversion detection, room temperature operation, KTP crystal

PACS: 42.60.–v, 42.65.–k, 87.50.U, 42.65.Dr

DOI: 10.1088/1674-1056/ae1c28 **CSTR:** 32038.14.CPB.ae1c28

1. Introduction

Terahertz (THz) wave refers to the electromagnetic wave with the frequency of 0.1 THz–10 THz (1 THz = 10^{12} Hz), which lies between infrared waves and microwaves. Because of its unique properties, THz wave has received rapidly growing attention in many application fields, such as non-destructive detection, medical imaging, and drug detection.[1–3] With the development of THz technology, THz detection systems with high sensitivity at room temperature have become a hot spot.

At present, the commonly used THz wave detectors can be divided into incoherent and coherent detectors. Incoherent detectors, such as bolometers, Golay cells and pyroelectric detectors, can detect the power or energy of THz waves through thermal response or pyroelectric effect. Especially, bolometers have high sensitivity of pJ level with liquid helium cooling down to low temperature of 4 K, which makes them complex and expensive.[4] Generally, the detection range of the incoherent detectors is relatively wide. But their response speed is slow, and the detection sensitivity cannot be achieved simultaneously under room temperature detection. Because of the characteristic of thermal response, these three THz detectors above can be easily affected by the environment, such as body heat and near-infrared laser. Recently, field effect transistors (FETs) based on complementary metal–oxide–semiconductor (CMOS) were developed with a noise equivalent power (NEP) of pW/Hz$^{1/2}$ level.[5] However, the detectable frequency is still limited below 1 THz. Terahertz optoacoustic array detectors based on ionic-liquid optoacoustics can reach a noise equivalent detection energy (NEDE) of 598 pJ with fast response speed of μs level.[6] But the detection frequency is also limited to be lower than 3 THz because of the THz source based on $LiNbO_3$ (LN) crystal. Coherent detectors can respond to the intensity of THz waves as well as frequency. In general, photoconductive sampling and electro-optical (EO) sampling are dependent on femtosecond lasers. The detectable THz frequency range is limited by the properties of photoconductive antennas and EO crystals.[7,8]

Optical frequency upconversion detection based on nonlinear frequency conversion can convert THz waves to near-infrared light through the input of pump laser and THz wave into nonlinear crystal simultaneously, where the frequency and intensity of near-infrared laser correspond to those of the input THz wave. It has the advantages of high sensitivity, wide dynamic range, and fast response.[9–11] Frequency upconversion detection based on difference frequency generation (DFG) has been proved as an effective method, which can realize a sensitive detection for the wide THz range of 1 THz–30 THz using organic crystals.[12,13] However, high detection sensitivity demands a high level of separation between the collinear signals of upconversion signal and pump signal. Frequency upconversion detection based on stimulated polariton scattering (SPS) has extremely high sensitivity because of the non-collinear separation of upconversion signal and pump signal.

[†]Corresponding author. E-mail: yuyewang@tju.edu.cn

© 2026 Chinese Physical Society and IOP Publishing Ltd. All rights, including for text and data mining, AI training, and similar technologies, are reserved.

Recently, a combination of parametric upconversion detection and single-photon counting technology has been developed to achieve a high sensitivity of 1.4 zJ at 2 THz.[14] However, the detection frequency based on LN crystal is usually limited below 3 THz because of the intrinsic oscillation frequency of LN. The $KTiOPO_4$ (KTP) crystal with multiple infrared- and Raman-active A1 phonon modes has great potential in realizing high frequency and high sensitivity detection. THz frequency ranges of 4.26 THz–4.50 THz and 4.80 THz–4.92 THz have been detected based on KTP crystal, where the minimum detectable energy was 2.35 fJ and the dynamic range reached 84 dB at 4.85 THz.[15] In order to improve the detection sensitivity, multi-stage noncollinear amplification by increasing gain length and collinear amplification with OPA have been developed. However, they also brought the issue of system complexity.

In this paper, a highly sensitive THz parametric upconversion detection has been realized based on a KTP crystal pumped by a 1064-nm pulsed laser. The relationship between the upconversion signal and spontaneous noise under different pump energies was investigated. The effects of pump energy on the detection sensitivity were studied in experiments. A minimum detectable energy of 57.6 aJ at 5.74 THz was obtained with a dynamic range of 104 dB, which gives an NEP of 147.8 $fW/Hz^{1/2}$. The THz frequency range of 5.24 THz–6.14 THz generated from the THz parametric generator has been detected.

2. Experimental setup

Figure 1 shows the schematic diagram of the THz parametric upconversion detector, which was basically composed of an injection pulse-seeded THz parametric generator (ips-TPG) and a THz parametric upconversion detector. A multimode Q-switched 1064-nm nanosecond laser with a repetition rate of 10 Hz and a pulse-width of 10 ns was chosen as the pump laser. A telescope system (T_1) was used to reduce the diameter of the pump beam to 4 mm. The pump laser was then divided into three beams by M_1 and M_4, which were successively called pump 1, pump 2, and pump 3. Pump 1 was used to generate a 532-nm laser, which was later used to generate a tunable pulse-seeder through an optical parametric oscillator (OPO) system. HWP_1 was used to adjust pump 1 to 45° polarization. A 532-nm laser was generated in KTP_1 with the second harmonic generation (SHG) of pump 1. The resonant cavity of the OPO system consisted of two plane-parallel mirrors M_6 and M_7, which were both coated with high reflection in the near-infrared band and high transmission at 532 nm. Type-II critical phase matching was achieved in the nonlinear gain medium KTP_2 ($\theta = 90°$, $\varphi = 24.5°$). The P-polarized signal wave was transmitted through a polarizing beam splitter (PBS) and resonated inside the cavity, and the S-polarized idler wave was highly reflected by the PBS and then injected into KTP_3 as a pulse-seeder. A combination of a half-wave plate (HWP_2)) and a Brewster plate (BP_1)) was used to adjust the energy of pump 2 and ensure the vertical polarization. Here, KTP_3 and KTP_4 were isosceles trapezoid crystals with longer and shorter bases of 39 mm and 22 mm, respectively. The thickness of the crystals along the z axis was 10 mm, and the angle between the base and the waist was 63°. Pump 2 and the pulse-seeder were injected into KTP_3 at a specific angle to satisfy the noncollinear phase-matching condition according to the wavelength of the two beams, which formed an ips-TPG system together as we reported before.[16] The THz wave was then focused to 4 mm and injected into KTP_4 through a pair of off-axis parabolic mirrors (OAP_1 and OAP_2)). After OAP_1 and OAP_2, the maximum energy of the THz wave before KTP_4 was 1.52 μJ/pulse, measured by a Golay cell (TYDEX, GC-1P) with a calibrated optical responsivity of 23 kV/W, which was the maximum THz wave energy for parametric upconversion detection. Several calibrated

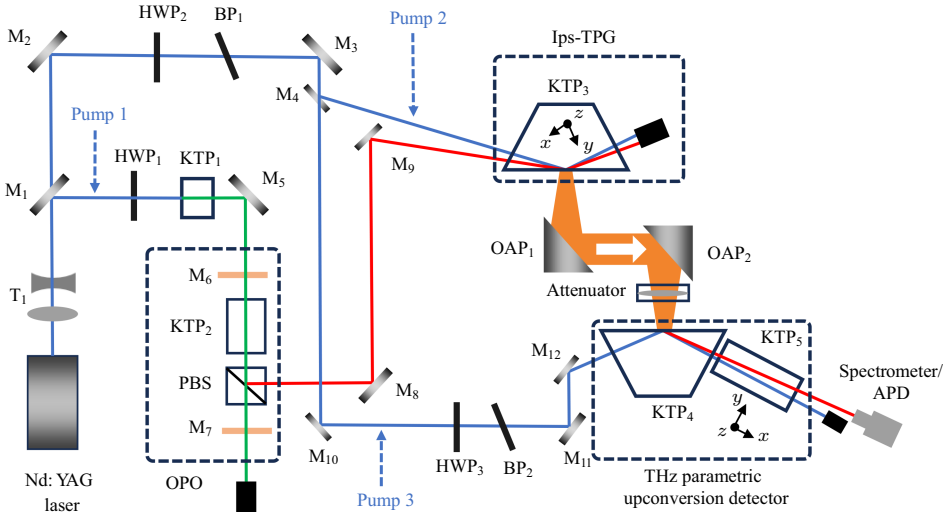


Fig. 1. Experimental setup of THz wave parametric upconversion detector.

black polyethylene plates with different thicknesses and transmittances were used as attenuator. Then, pump 3 and the THz wave were injected into KTP_4 according to the noncolinear phase-matching condition and the upconversion signal was generated based on SPS in KTP_4. KTP_5 (10 mm×12 mm×44 mm) was placed after KTP_4 as the secondary stage to amplify the upconversion signal. The upconversion signal was finally detected by highly sensitive spectrometer, InGaAs PIN diode (PD) and InGaAs avalanche photon diode (APD). It should be mentioned that, although the propagation direction of upconversion signal was different from that of pump laser, the scattered 1064-nm near-infrared laser could still enter into APD, which could make APD saturation. Thus, a set of 6 filters (CHROMA, RET1072lp) with an optical distinction value of 7 was applied in front of APD.

3. Results and discussion

When only pump 3 is injected into KTP_4, a broadband spontaneous noise will be generated due to the parametric effect as the pump intensity (P) exceeds the spontaneous noise threshold (P_{sp}). When the pump intensity is strong enough to exceed the SPS threshold (P_{sps}), Stokes light and THz wave will be generated simultaneously based on TPG. In the process of upconversion detection, THz wave and pump 3 are injected into KTP_4 simultaneously at the angle that satisfies noncolinear phase matching condition. The THz wave will be upconverted to near-infrared light. Due to the upconversion process and spontaneous parametric process both satisfying the noncollinear phase matching condition, the upconversion signal and the spontaneous noise with equal wavelengths are spatially coincident at the same position. Considering the threshold of upconversion process (P_{up}) is commonly lower than that of spontaneous noise generation, the energy of pump laser was set at lower level to suppress the influence of spontaneous noise in our previous report.[15] However, during the second order parametric amplification process, low pump energy also causes low upconversion signal intensity, which leads to low detection sensitivity. The feasibility of improving detection sensitivity under higher pump energy is still not clear until now. In order to increase the parametric gain effectively, it is necessary to clarify the intensity relationship between spontaneous noise and upconversion signal during the pump energy enhancement process.

The THz frequency of 5.7 THz from ips-TPG was chosen for parametric upconversion detection due to the strong Raman scattering intensity of the polariton formed by optical phonon modes with vibration frequency of 202 cm^{-1} in KTP crystal, whose frequency shift is 190 cm^{-1}. In other words, there is strong gain in the process of THz parametric upconversion based on KTP crystal at 5.7 THz. At the same time, it is easy to obtain spontaneous noise with lower pump energy. In this case, the wavelength of the pulse-seeder produced by the OPO system was set to be 1086.54 nm through angle-tuning in KTP_2. Figure 2 shows the wavelengths of the upconversion signal, Stokes wave, and seed wave from ips-TPG under the input THz wave energy of 1.52 μJ/pulse and the pump energy of 30 mJ, where the spontaneous parametric signal could not be measured by the spectrometer. The wavelength of the upconversion signal was consistent with those of the seed wave and Stokes wave (1086.54 nm), which proves the frequency detection accuracy of THz parametric upconversion detector. Then, the spontaneous parametric signal was measured without THz input under the pump energy of 50 mJ, which was shown by the green curve in Fig. 2. It can be seen that the central wavelength of broadband noise coincided with the upconversion signal. It should be noticed that although there are four curves in Fig. 2, the green curve of spontaneous noise was from a different experimental setup compared with the other three curves. Besides, because of the differences in position and propagation direction, it is difficult to ensure the same coupling efficiency of the four beams into the spectrometer. Therefore, the measurement spectra of the four beams cannot fully reflect the relative intensity.

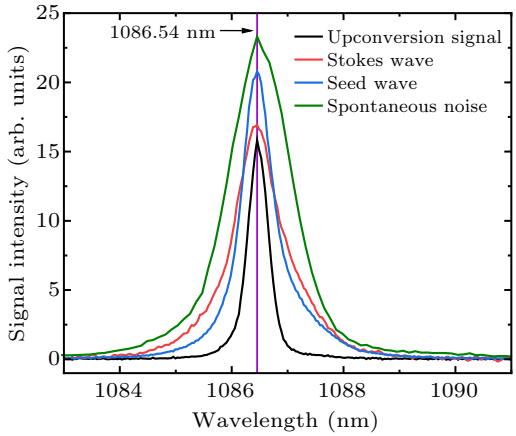


Fig. 2. Spectra of upconversion signal, Stokes wave, seed wave, and spontaneous noise.

Then, PD or APD was placed at the overlapping area between the upconversion signal and the spontaneous noise signal after KTP_5, as shown in Fig. 3(a). In practical observation, the spontaneous noise signal usually appears as an arc or a bow shape on the detector card, while the upconversion signal usually appears as a circle and lies inside the spontaneous noise. The area of spontaneous noise is relatively larger than that of the upconversion signal due to the broadband characteristic of noise. Figure 3(b) shows the measurement results of PD/APD with and without the input of THz wave under different pump energies, where part A, part B, and part C were measured by APD because of the low signal intensity, and part D was measured by PD. When THz wave was not injected into KTP_4, the detected signal of PD/APD referred to the intensity of ambient and spontaneous noise.

When THz wave was injected into KTP_4, the measured signal was a mixture of upconversion signal, ambient noise, and spontaneous noise signal. Here, the THz wave energy was set to be 1.52 μJ/pulse. In part A, the pump energy was below 17 mJ, which was lower than P_{sp} and P_{up}. It could not trigger the spontaneous process or the upconversion process. The intensity of APD was completely from ambient noise. In part B, the pump energy was increased to a maximum of 32 mJ, which satisfied the relationship of $P_{up} < P < P_{sp}$. The upconversion signal can be detected with THz wave input, which led to the increase of APD signal intensity. Moreover, the upconversion signal intensity was increased linearly with the pump energy increment. Comparatively, the APD signal was still completely composed of ambient noise without THz input, where the intensity was almost the same as the value in part A. In part C and part D, pump energy was gradually raised to 127 mJ, which was higher than both P_{sp} and P_{up}; the upconversion signal and spontaneous noise were both generated. It can be seen that the signal intensities from APD (PD) with and without THz input both showed linear relationships with the pump intensity when the pump energy was larger than 32 mJ. Considering ambient noise is relatively low, the APD (PD) signal with THz input was mainly composed of upconversion signal and spontaneous noise signal. The data in Fig. 3(b) deserve further analysis. The slope of the red curve in parts C and D is measured to be 2.13 /mJ, which was all from spontaneous noise. The slope of the black curve in parts C and D is measured to be 4.83 /mJ, which was from upconversion signal and spontaneous noise. The difference of these two slopes was 2.70 /mJ, which is contributed by upconversion signal, meaning that upconversion signal increased more rapidly than spontaneous noise as pump energy exceeded 32 mJ. The slope of the black curve in part B is measured to be 3.23 /mJ, which was all from upconversion signal because pump energy is lower than P_{sp}. The slope of the black curve contributed by upconversion signal decreases when pump energy exceeds 32 mJ, which means that the conversion rate from pump to upconversion signal decreases because of the present of spontaneous noise. Thus, it can be deduced that, although the spontaneous noise signal was increased with the increase of pump energy, the pump energy was mainly used for the generation of upconversion signal with THz input. The impact of spontaneous noise can be avoided by the subtraction of the intensities of the two signals with and without THz wave input. Therefore, the THz parametric upconversion detection sensitivity could be improved through increasing the pump energy in a certain range.

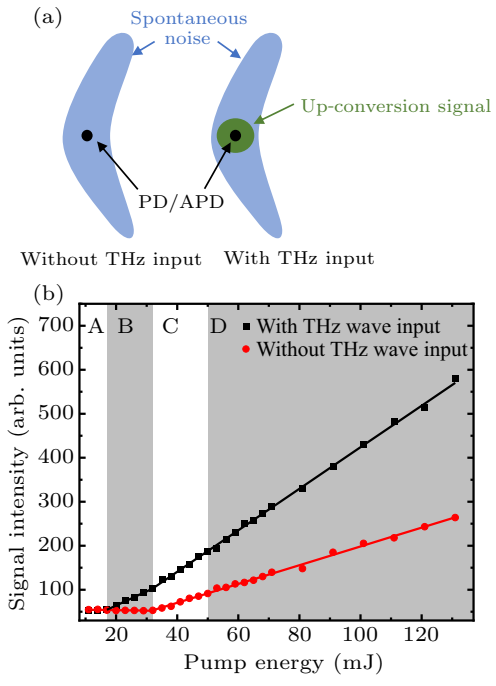


Fig. 3. (a) Schematic diagram of upconversion signal and noise measurements by PD/APD. (b) The detected signal of PD/APD under different pump energies with and without THz wave input.

In order to determine the best detection sensitivity of the THz parametric up-conversion detection system under higher pump energy, the relationship between pump energy and minimum detectable THz wave energy was investigated. Firstly, the intensity of upconversion signal under different THz wave energy input was investigated, where the output of APD was 512 times averaged for every measurement to reduce the influence of pump energy fluctuation. The pump energy was set to be 127 mJ and the THz wave energy was attenuated with multiple attenuators. Figure 4 shows the upconversion signal intensity versus the input THz wave energy, where the intensity of upconversion signal was the difference of the APD signals with and without THz wave input. It can be seen that the upconversion signal intensity showed a linear relationship with the input THz intensity. In order to obtain the accurate minimum detectable THz wave energy, the abscissa interval was taken smaller near the minimum terahertz wave energy. It can be seen that the minimum detectable energy is 57.6 aJ with pump energy of 127 mJ. Then, the experimental procedure was repeated under a wide range of pump energy in order to investigate the relationship between pump energy and minimum detectable energy, as shown in Fig. 5. The minimum detectable THz wave energy of this system within the pump energy range of 23 mJ–127 mJ was obtained as 57.6 aJ with the pump energy of 127 mJ. Considering the maximum THz wave energy was 1.52 μJ/pulse, the dynamic range of the THz detection system was 104 dB and the NEP was 147.8 fW/Hz$^{1/2}$. The detection sensitivity of this system was 7 orders of magnitude higher than that of Golay cell and 3 orders of magnitude higher than that of bolometer. Meanwhile, it can be seen that the curve has several inflection points. Similarly, the abscissa interval was taken smaller at the turning part of the curve. When the pump energy was between 23 mJ and 32 mJ, which

satisfied the relationship of $P_{up} < P < P_{sp}$, the minimum detectable THz wave energy was decreased as the pump energy was increased because of the absence of spontaneous noise, as shown in part a of Fig. 5. It was consistent with our previous reports.[15,17] When the pump energy was between 32 mJ and 38 mJ, the pump energy was mainly consumed to generate spontaneous noise. Thus, the minimum detectable THz wave energy showed a steep increase, as shown in part b of Fig. 5. When the pump energy was continuously increased, the gain of the upconversion signal was greater than that of the spontaneous noise. Therefore, the minimum detectable THz wave energy was monotonically decreased as the pump energy was increased.

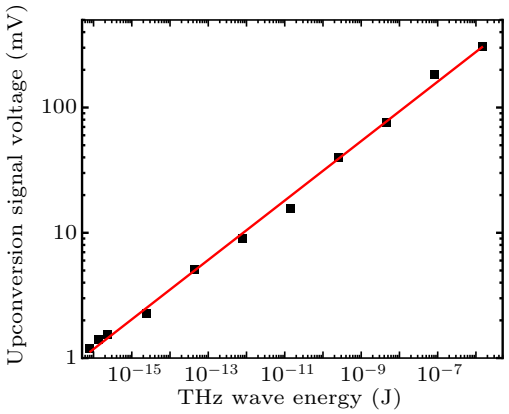


Fig. 4. Upconversion signal intensity as a function of the input THz wave energy.

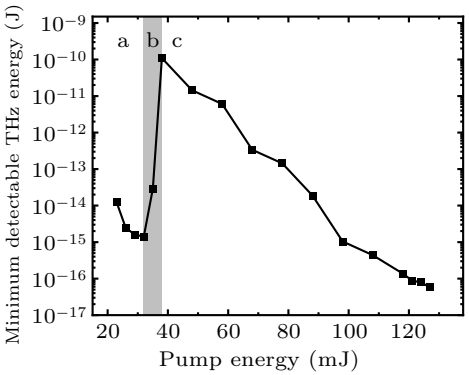


Fig. 5. Minimum detectable THz wave energy as a function of pump energy.

Finally, the detection performance of the system at different frequencies was studied. Figure 6(a) shows the measured spectra of the upconverted signals at different wavelengths from 1084.6 nm to 1088.1 nm, corresponding to the THz frequency range of 5.24 THz to 6.14 THz. The minimum detectable THz wave energy and the best pump energy at different frequencies are shown in Fig. 6(b). Away from 5.74 THz, the detection sensitivity was decreased due to being far from the strong vibration mode and the decreased parametric gain. Correspondingly, the optimized pump energy for detection sensitivity was increased. Figure 6(c) shows the temporal profile of the upconversion signal measured by APD. The pulse width at the half maximum was measured to be 2.4-ns full-width. Assuming that the upconversion signal satisfies a Gaussian distribution, the pulse width of the THz wave can be estimated as 2.5 ns.[18]

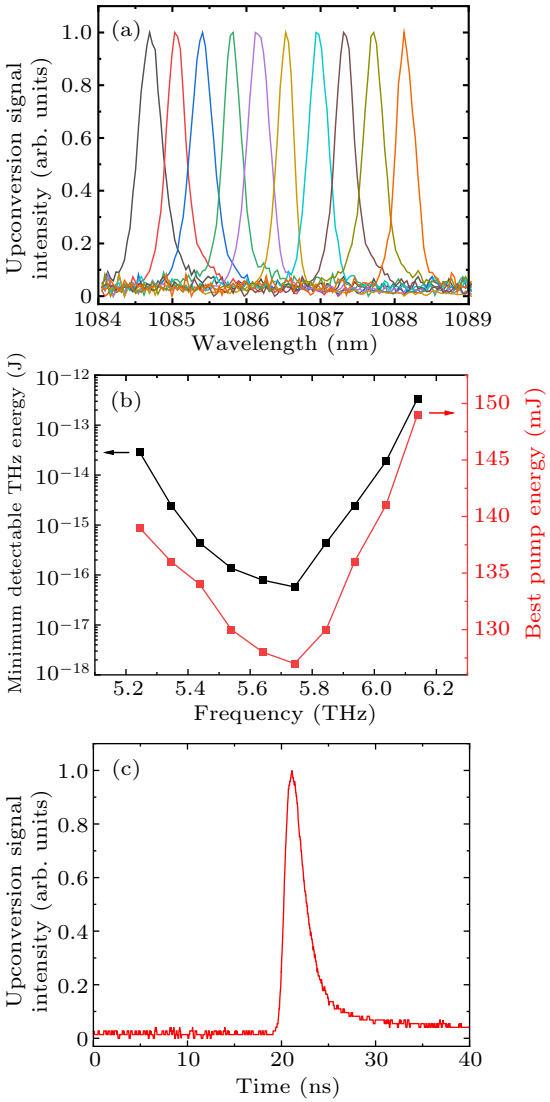


Fig. 6. (a) The frequency detection range of parametric upconversion detection. (b) The minimum detectable THz wave energy and the best pump energy as a function of frequency. (c) Temporal profile of upconversion signal.

4. Conclusion

In this work, a high-sensitivity THz parametric upconversion detector based on KTP crystal was investigated. The effects of pump energy on the THz detection sensitivity were studied in experiment, where the upconversion signal and spontaneous noise were both amplified linearly with the increase of pump energy. The minimum detectable energy of 57.6 aJ and a dynamic range of 104 dB at 5.74 THz were achieved at the pump energy of 127 mJ/pulse, which was three orders of magnitude higher than that of bolometer. Furthermore, this system can achieve high detection sensitivity over a wide frequency range of 5.24 THz–6.14 THz. This kind of THz upconversion detection technology using a KTP crys-

tal under high pump energy not only realizes the detection of extremely weak THz wave, but also expands the frequency upper limit of parameter upconversion detection.

Acknowledgements

Project supported by the National Natural Science Foundation of China (Grant Nos. 62175182, U22A20353, 62275193, and 62575210) and the Young Scientific and Technological Talents (Level Two) in Tianjin (Grant No. QN20230204).

References

[1] Shirkavand A, Tuchin V V, Jahangiri F and Mohajerani E 2020 *Opt. Quantum Electronics* **54** 467

[2] Taylor Z D, Singh R S, Culjat M O and Culjat J 2008 *Opt. Lett.* **33** 1258

[3] Takida Y, Nawata K, Suzuki S, Asada M and Minamide H 2017 *AIP Adv.* **7** 035020

[4] Richards P L 1994 *J. Appl. Phys.* **76** 1

[5] Zhang X, Fu H P, Ma K X, Yan N N, Liu Y X and Mu Y P 2023 *IEEE Trans. Terahertz Sci. Technol.* **13** 464

[6] Yao Y X, Wang K, Du K P, Zhang C S, Li J and Tian Z 2025 *Chin. Opt. Lett.* **23** 083701

[7] Pradarutti B, Matthäus G, Riehemann S, Notni G and Tünnermann A 2008 *Opt. Commun.* **281** 5031

[8] Ito H, Nakajima F, Ohno T, Furuta T, Nagatsuma T and Ishibashi T 2008 *Jpn. J. Appl. Phys.* **47** 6256

[9] Babin A A, Petryakov V N and Freidman G I 1983 *Sov. J. Quantum Electronics* **13** 958

[10] Kong W P, Yan Q, Li Z Y, Zou M, Zhou X and Qin Y 2021 *IEEE T. Thz. Sci. Technol.* **11** 389

[11] Mine S, Kawase K and Murate K 2021 *Opt. Lett.* **46** 2618

[12] Qi F, Fan S, Notake T, Nawata K, Matsukawa T, Takida Y and Minamide H 2014 *Laser Phys. Lett.* **11** 085403

[13] Guo Q X 2024 *Research on highly sensitive terahertz wave detection technique and terahertz parametric source based on nonlinear frequency conversion*, Ph. D. Dissertation (Qingdao: Shandong University) (in Chinese)

[14] Fandio D J J, Vishnuradhan A, Yalavarthi E K, Wei C, Couture N, Gamouras A and Ménard J M 2024 *Opt. Lett.* **49** 1556

[15] Wang Y Y, Hu C H, Chen K, Yan C, Xu D G, Takida Y, Minamide H and Yao J Q 2022 *Opt. Lett.* **47** 5853

[16] Chen K, Tang L H, Xu D G, Wang Y Y, Yan C, Nie G, Hu C, Wu B, Zhu J and Yao J 2021 *ACS Photon.* **8** 3141

[17] Wang Y Y, Nie G, Hu C, Chen K, Yan C, Wu B, Zhu J F, Xu D G and Yao J Q 2022 *Chin. Phys. B* **31** 024204

[18] Qi F, Fan S, Notake T, Nawata K, Matsukawa T, Takida Y and Minamide H 2014 *Opt. Lett.* **39** 1294